FEBS Letters

FEBS PRESS
science publishing by scientists

LncRNA H19 functions as a competing endogenous RNA to regulate AQP3 expression by sponging miR-874 in the intestinal barrier

Zhaoran Su[1,2,*], Xiaofei Zhi[3,*], Qun Zhang[1,3,*], Li Yang[1], Hao Xu[1] and Zekuan Xu[1]

1 Division of Gastrointestinal Surgery, Department of General Surgery, The First Affiliated Hospital of Nanjing Medical University, China
2 Division of Gastrointestinal Surgery, Department of General Surgery, The People's Hospital of Tongling City, China
3 Department of General Surgery, The Affiliated Hospital of Nantong University, China

Correspondence
H. Xu and Z. Xu, Division of Gastrointestinal Surgery, Department of General Surgery, The First Affiliated Hospital of Nanjing Medical University, 300 Guangzhou Road, Nanjing 210029, China
Fax/Tel: +86 025 83781992
E-mails: brightmoon01@sina.com and xuzekuan@njmu.edu.cn

*These authors contributed equally to this study.

(Received 29 January 2016, revised 12 March 2016, accepted 29 March 2016, available online 17 April 2016)

doi:10.1002/1873-3468.12171

Edited by Lukas Alfons Huber

Intestinal barrier dysfunction is a significant clinical problem, which develops in a variety of acute or chronic pathological conditions. In a previous study, we found that microRNA-874 (miR-874) suppresses aquaporin-3 (AQP3) expression, which contributes significantly to intestinal barrier dysfunction. Recently, a new regulatory circuit was identified in which RNA can crosstalk with each other by competing for shared miRNA. Here, we show that the human long noncoding RNA (lncRNA) H19 may function as a competing endogenous RNA (ceRNA) to regulate the expression of AQP3 through competition for miR-874, thus playing a significant role in maintaining intestinal barrier function.

Keywords: MicroRNA; Long non-coding RNA; Intestinal barrier

The intestinal barrier, which consists of mechanical, biological, immunological and chemical barriers, plays a central role in maintaining internal homeostasis [1]. Intestinal barrier dysfunction is observed in a variety of acute or chronic pathological conditions, such as trauma, ischaemia, inflammatory bowel diseases (IBD), total parenteral nutrition (TPN) and intestinal obstruction [2–4]. Several lines of evidence support the concept that intestinal barrier dysfunction may increase the intestinal permeability, which often causes fatal conditions, including sepsis and multiple organ failure, resulting in a high degree of morbidity and mortality [4,5]. Although many investigations have focused on the regulatory mechanisms of intestinal mucosal barrier function under different pathological conditions, the underlying molecular mechanisms of intestinal barrier dysfunction remain poorly understood.

miRNA are ~ 20 nucleotide long regulatory noncoding RNA that are initially expressed as hairpin transcripts of primary miRNA and play an important role in modulating the activity of thousands of genes by translational repression or promoting RNA degradation [6–8]. Our previous studies found that miR-874 suppressed aquaporin-3 (AQP3) expression by binding to the 3′UTR of AQP3 mRNA in Caco-2 cells [9].This downregulation of AQP3 significantly impaired the intestinal barrier integrity via opening the tight junction complex, which may promote intestinal barrier dysfunction [10].

Abbreviations
ceRNA, competing endogenous RNA; IHC, immunohistochemistry; lncRNA, long noncoding RNA; LY, lucifer yellow; PBS-T, PBS containing 0.05% Tween 20; qRT-PCR, quantitative real-time PCR; SMA, superior mesenteric artery; TEER, transepithelial electrical resistance.

Long noncoding RNA (lncRNA), defined as noncoding RNA more than 200 nucleotide in length, were once considered to be simply transcriptional 'noise' or cloning artefacts in past decades [11]. However, recent studies demonstrated lncRNA may function as competing endogenous RNA (ceRNA) that 'sponge' miRNA, thereby modulating the derepression of miRNA targets and imposing an additional level of post-transcriptional regulation [12,13]. lncRNA H19 was discovered in 1991 by Bartolomei *et al*. [14] and was first described as a tumour suppressor, but more recent analysis shows that H19 plays an important role in a wide range of biological processes, including proliferation, cell cycle, apoptosis, differentiation and invasion [15–19].

In this study, we report that lncRNA H19 downregulation is a characteristic molecular change in intestinal barrier dysfunction and investigate the biological roles of H19 on the intestinal barrier. Moreover, mechanistic analysis reveals that H19 may function as a ceRNA to regulate the expression of AQP3 through competition for miR-874, thus playing a protective role in the intestinal barrier. The present work provides the first evidence for a correlation between miR-874, H19 and AQP3, shedding new light on the treatment of intestinal barrier dysfunction.

Materials and methods

Patient samples

Paired specimens of proximal mucous tissues and distal mucous tissues of lesion locations were obtained from 39 adhesive small-bowel obstruction patients who had undergone partial excision of the small bowel at Nanjing Medical University Affiliated First Hospital, between February 2011 and May 2014. Samples were immediately frozen in liquid nitrogen. This study was approved by the Ethics Committee of the First Affiliated Hospital of Nanjing Medical University, and every patient provided written informed consent. The study methodologies conformed to the standards set by the Declaration of Helsinki.

Mouse model of intestinal ischaemia reperfusion injury

All procedures and animal care were approved by the institutional animal care and use committee of Nanjing Medical University followed internationally recognized guidelines. A total of 40 eight-week-old C57BL/6 mice (Chinese Academy of Sciences, Shanghai, China) were randomly divided into sham group, 15, 30 and 45 min occlusion group. The mouse abdominal cavity was opened after intraperitoneal anaesthesia using 40 $mg \cdot kg^{-1}$ pentobarbital. By using nontraumatic vascular clamps, the superior mesenteric artery (SMA) was occluded for 15, 30 or 45 min with 5 min reperfusion in each ischaemic group. The animals in the sham group underwent laparotomy without SMA occlusion. After the above procedures, 10 cm of jejunum was obtained for immunochemistry, western blot, quantitative real-time PCR (qRT-PCR) and miRNA PCR analyses.

Cell culture assays

Human Caco-2 cells were purchased from the Chinese Academy of Sciences and routinely cultured in DMEM (Gibco, Carlsbad, CA, USA) containing 1% nonessential amino acids (Gibco, Montevideo, Uruguay) and 10% fetal bovine serum (Gibco, Montevideo, Uruguay) at 37 °C with 5% CO_2. To form the Caco-2 monolayer, 2.0×10^5 Caco-2 cells were seeded onto the apical chamber of a Transwell bicameral chamber containing 0.4 μm pores and were grown for 14 days to reach confluence and fully differentiate. An intestinal ischaemia model *in vitro* was established by incubating the Caco-2 cells in anaerobic chambers (Thermo Scientific, 37 °C, 10% CO_2, 1% O_2) with serum-free conditions. The cell line has been tested and authenticated.

Lentivirus production and cell transfections

Two complementary oligonucleotides of small hairpin RNA targeting the 5′-CGTGACAAGCAGGACATGA-3′ sequence were chemically synthesized, subcloned into the GV115 lentiviral vector (GenePharma, Shanghai, China) and transfected into Caco-2 cells to generate Caco-2/siH19. A hairpin siRNA with no sequence homology to human genes provided by the manufacturer (GenePharma) was used as the negative control (siH19NC). For overexpression, the full-length H19 complementary DNA was subcloned into the GV299 lentiviral vector (GenePharma) and transfected into Caco-2 cells to generate Caco-2/H19, and the GV299 empty lentiviral construct (GenePharma) was used as a negative control (H19NC) for H19 overexpression. We also modified the commercial LV3-has-miR-874-pre-microRNA vector (pre-miR-874) and LV3-has-miR-874-sponge inhibitor vector (miR-874 inhibitor) from GenePharma. LV3 empty lentiviral construct (miR-NC) served as a negative control (GenePharma). Briefly, the vectors described above were used to infect cells at an appropriate multiplicity of infection (MOI) when Caco-2 cells had grown to 20–30% confluence by using Lipofectamine 2000 (Invitrogen, Carlsbad, CA, USA) for 24 h. Then, stable cell lines were selected using 3 $\mu g \cdot mL^{-1}$ bulk puromycin-resistant culturing (puromycin; Sigma, St Louis, MO, USA) for 5 days. After that, cells were subjected to RNA/protein extraction and further functional assays.

Luciferase assay

Caco-2 cells (2.0×10^4) were cultured in 96-well plates and transfected with 150 ng of either miR-874 or empty vector together with 50 ng of firefly luciferase reporter carrying the 3′UTR of AQP3, wild-type or mutant H19 fragment, and 2 ng of pRL-TK (Promega, Madison, WI, USA) using Lipofectamie 2000 (Invitrogen). rno-miRNA-344 (GenePharma) acts as a negative control. At 48 h post-transfection, relative luciferase activity was calculated using a luciferase assay kit (Promega) according to the manufacturer's instructions. The transfection was repeated in three times.

qRT-PCR and miRNA RT-PCR

Total RNA was extracted from frozen tissues and cells using TRIzol reagent (Invitrogen), and reverse transcription using Moloney murine leukaemia virus (M-MLV) reverse transcriptase (Promega) was carried out according to the manufacturer's instructions. qRT-PCR was performed using a 7500 Real-Time PCR System (Applied Biosystems, Carlsbad, CA, USA) with Fast Start Universal SYBR Green Master (Roche, San Francisco, CA, USA). β-actin was used as a reference for lncRNA. The gene-specific primers were as follows: H19 (forward: 5′-ATCGGTGCCTCAGCGTTCGG-3′; reverse: 5′-CTGTCCTCGCCGTCACACCG-3′); β-actin (forward: 5′-TCATGAAGTGTGACGTGGACAT-3′; reverse: 5′-CTCAGGAGGAGCAATGATCTTG-3′). Target-specific reverse transcription and Taqman microRNA assay probes were assayed using the Hairpin-it™ miRNA qPCR Quantitation Kit (GenePharma), according to the manufacturer's instructions. The reactions were also performed using the 7500 Real-Time PCR System. The snRNA U6 was selected as an endogenous reference for miRNA. Data analysis was performed using the $2^{-\Delta Ct}$ method. All experiments were performed independently in triplicate.

Western blot assay

Antibodies against AQP3 (Abcam, Cambridge, MA, USA, 1 : 500 dilution), claudin-1 (Cell Signaling Technology, Boston, MA, USA 1 : 400 dilution), occludin (Abcam, 1 : 400 dilution), claudin-2 (Abcam, 1 : 500 dilution), ZO-1 (Cell Signaling Technology, 1 : 1000 dilution), E-cadherin (Cell Signaling Technology, 1 : 500 dilution), beta-catenin (Cell Signaling Technology, 1 : 500 dilution) and GAPDH (Abcam, 1 : 1000 dilution) were used. Western blot assays were carried out as previously described [9].

Immunohistochemistry

All specimens were fixed in 4% formalin for 24 h and then embedded in paraffin. MaxVision™ techniques (Maixin-Bio, Shanghai, China) were used for immunohistochemistry (IHC) according to the manufacturer's instruction. After blocking the endogenous peroxides and proteins, 4 μm sections were incubated overnight at 4 °C with diluted primary antibodies specific for AQP3 (Abcam, 1 : 200 dilution). Next, the slices were incubated with HRP-polymer-conjugated secondary antibody at 37 °C for 1 h. Then, the slices were stained with a 3,3′-diaminobenzidine solution for 3 min and counterstained with haematoxylin. The images were then scored according to the staining depth as previously described [20].

Immunofluorescence

After cell transfections, Caco-2 cells were washed with 0.1 mol·L^{-1} HEPES containing Immunol Staining Fix Solution (Beyotime, Shanghai, China) for 15 min after culturing to 20% confluence. After washes in Immunol Staining Wash Buffer (Beyotime), the fixed cells were blocked in Immunol Staining Blocking Buffer (Beyotime) for 60 min at room temperature. After overnight incubation at 4 °C with primary AQP3 antibody at a dilution of 1 : 200 (Abcam), the cells were incubated with PE-labelled goat anti-(mouse secondary antibodies) (Beyotime) at 37 °C for 80 min after washing 5× with PBS containing 0.05% Tween 20 (PBS-T). The cells were then washed again 5 times for 10 min with PBS-T, and the nuclei were counterstained with diaminophenylindole (0.5 μg·mL^{-1}) for 5 min. Cells were visualized under a fluorescence microscope (Nikon, Tokyo, Japan) using Axio Vision software.

RNA-binding protein immunoprecipitation (RIP) assay

We performed RIP experiments using the Magna RIP kit (Millipore, Bedford, MA, USA), according to the manufacturer's protocol. Briefly, Caco-2 cells were scraped off and lysed in complete RIP lysis buffer at 50% confluency. Then, 100 μL of whole cell extract was incubated with RIP buffer containing magnetic beads conjugated with human anti-(Ago2) antibody (Millipore) or normal mouse IgG (negative control; Millipore). After digesting the protein by incubating with proteinase K, immunoprecipitated RNA was isolated and purified. Then, qRT-PCR analysis was performed to demonstrate the presence of the binding targets.

Measurement of the transepithelial electrical resistance

A Millicell electrical resistance system (Millipore) was used to measure the transepithelial electrical resistance (TEER) of the Caco-2 cell monolayer at 7, 11, 21 and 28 days after seeding.

Bacterial translocation and paracellular permeability

When the Caco-2 cell monolayer had grown in culture for 14 days, an inoculum containing 10^5 bacterial cells (*E. coli*

C25) was added to the apical side. At 20, 40, 120, and 180 min after adding bacteria, bacterial translocation was measured by quantitatively culturing samples of medium (100 μL) obtained from the basal chamber.

Paracellular permeability was assessed by measuring the flux of lucifer yellow (LY) from apical to basal chambers of the Transwell as described previously [9].

Statistical analysis

Statistical analysis was performed using SPSS ver. 11.0 for Windows (SPSS Inc., Chicago, IL, USA). All continuous variables were expressed as the mean ± SD, and comparison analysis was performed with paired and unpaired Student's *t*-test and analysis of variance (ANOVA). *P*-values < 0.050 were considered statistically significant.

Results

lncRNA H19 controls the miR-874 targeting AQP3

Among the many targets of miR-874, we concentrated on AQP3 because several lines of evidence supported the concept that AQP3 protein plays a key role in maintaining intestinal barrier function [10,21]. Furthermore, our previous studies revealed that miR-874 decreased AQP3 expression in Caco-2 and gastric cancer cells by targeting its 3′UTR [9,22]. To investigate whether the expression of miR-874 is regulated by lncRNA, Diana Tools (http://diana.imis.athena-innovation.gr/) and Segal Lab (http://genie.weizmann.ac.il/) were used in combination to predict lncRNA which might target miR-874. As shown in Fig. 1A, bioinformatics analysis revealed a putative lncRNA, lncRNA H19, containing a putative 7-mer-binding motif binding site within miR-874.

The lncRNA H19 was cloned downstream of the luciferase gene and named RLuc-H19-WT and then transfected together with miR-874-coding plasmids. The results showed that luciferase activity was reduced by ~ 50% compared with the empty vector control when miR-874 was expressed (Fig. 1B). Then, we mutated the putative miR-874 binding site by site-directed mutagenesis, resulting in RLuc-H19-Mut (Fig. 1A). As expected, suppression of luciferase activity was completely abolished in this mutant construct compared with wild-type vector (Fig. 1B). The 3′UTR of AQP3 was fused to the luciferase coding region (RLuc-AQP3 3′UTR) and transfected with plasmids encoding miR-874 and an empty plasmid vector. rno-miRNA-344 acted as a negative control. The luciferase assay showed that miR-874 significantly inhibited luciferase activity of the RLuc-AQP3 3′UTR reporter. Then, RLuc-AQP3 3′UTR was subsequently transfected together with plasmids encoding miR-874 and H19 (pCDNA/H19). Luciferase assays indicated that, in the presence of H19, RLuc-AQP3 3′UTR repression was restored compared with the control group (Fig. 1C).

miRNA ribonucleoprotein complexes (miRNPs) contain Ago2 protein, the core component of the RNA-induced silencing complex (RISC) and miRNA are known to be present in the cytoplasm in the form of miRNPs [23,24]. After treatment with a miR-874 inhibitor and miR-NC, respectively, RIP experiments were performed on Caco-2 cell extracts using antibodies against Ago2. The results found that H19 and miR-874 were preferentially enriched in Ago2-containing miRNPs relative to control immunoprecipitates (IgG). When we down-regulated the level of miR-874 in Caco-2 cells, the level of H19 was significantly reduced in immunoprecipitates (Fig. 1D).

To investigate the impact of H19 and miR-874 on AQP3 expression in Caco-2 cells, we performed both overexpression and knockdown experiments. H19 knockdown in Caco-2 cells resulted in the up-regulation of the miR-874 (Fig. 1E) and down-regulation of the AQP3 protein compared with the negative control (Fig. 1F,G). Conversely, the level of miR-874 was significantly reduced (Fig. 1E) and the protein level of AQP3 was significantly increased in Caco-2 cells following overexpression of H19 (Fig. 1F,G). The results of rescue experiment indicated that the positive relationship between H19 and AQP3 could be reverted by overexpression and knockdown of miR-874 in Caco-2 cells (Fig. 1F).

H19, miR-874 and AQP3 expression in adhesive small-bowel obstruction tissues

To evaluate the expression pattern of miR-874 and lncRNA H19 in human disease small-bowel mucous samples, we employed qRT-PCR in 39 pairs of mucous tissues proximal and distal to lesion locations obtained from adhesive small-bowel obstruction patients who had undergone partial excision of the small bowel. The results indicated that miR-874 was significantly up-regulated and H19 was significantly down-regulated in proximal compared with the distal tissues of diseased small-bowel mucous (Fig. 2A,B). Thirty-eight of 39 (97%) were significantly reduced in proximal tissues of diseased small-bowel mucous compared with matched distal tissues. The AQP3 protein expression of nine random matched samples is shown in Fig. 2C. We also found a relationship between the

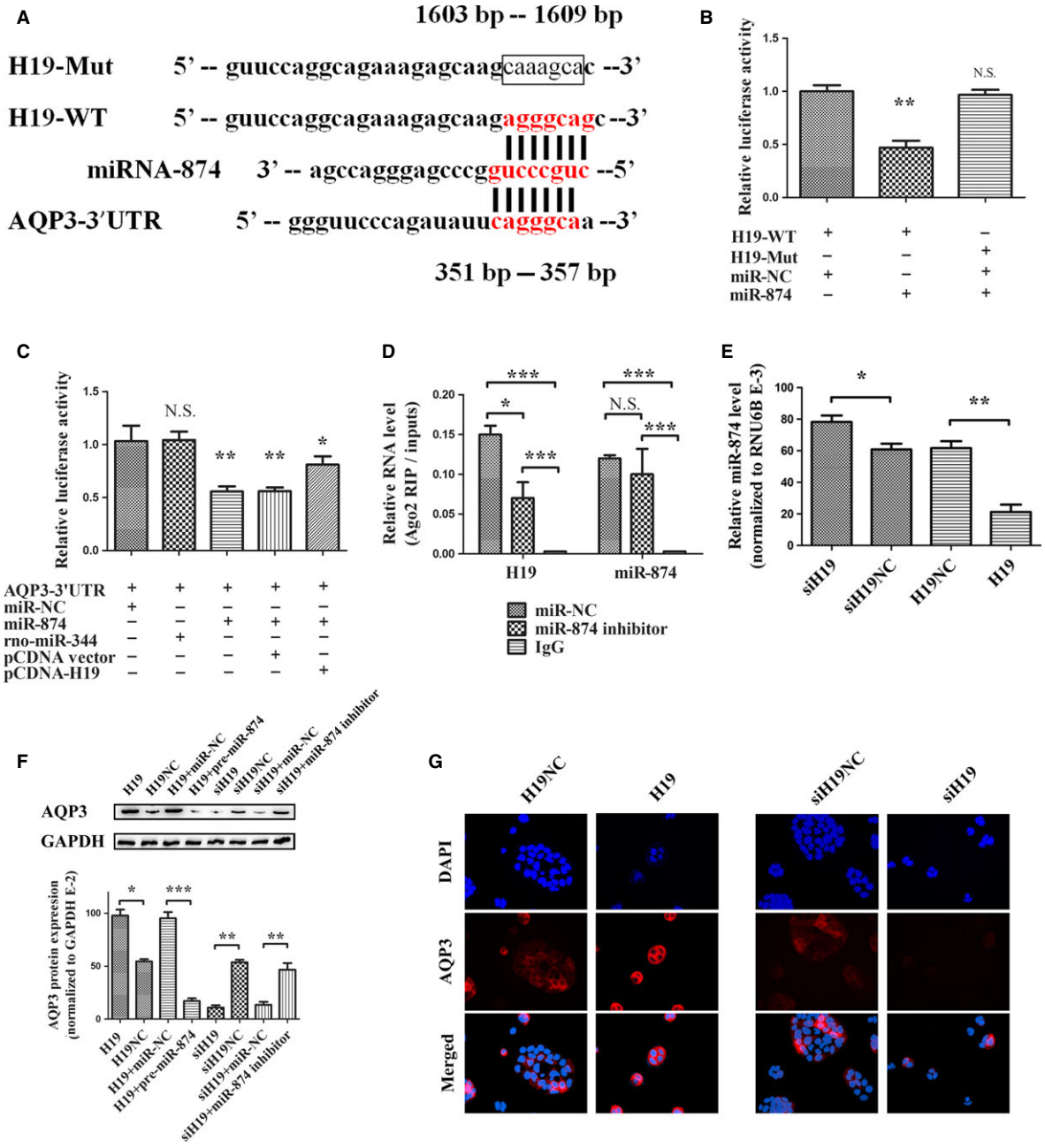

Fig. 1. lncRNA H19 controls the miR-874 targeting AQP3. (A) Bioinformatics analysis revealed a putative 7-mer-binding motif within lncRNA H19 and the AQP3 3′UTR regions which contains the binding site for miR-874. Mutant H19 (H19-Mut) was generated by mutating the putative miR-874 binding site. (B) The luciferase reporter plasmid containing wild-type or mutant H19 was cotransfected into Caco-2 cells with miR-874 in parallel with an empty plasmid vector. Luciferase activity was determined using the dual luciferase assay and shown as the relative luciferase activity normalized to *Renilla* activity. The histogram indicates the values of luciferase measured 48 h after transfection. (C) The 3′UTR of AQP3 was fused to the luciferase coding region (RLuc-AQP3 3′UTR) and transfected in Caco-2 cells with miR-874 to confirm AQP3 is a target of miR-874. RLuc-AQP3 3′UTR and miR-874 constructs were cotransfected into Caco-2 cells with plasmids expressing H19 (pCDNA/H19) or with a control vector to verify the ceRNA activity of H19. rno-miRNA-344 was used as a negative control. The histogram indicates the values of luciferase measured 48 h after transfection. (D) RIP with mouse monoclonal anti-(Ago2), preimmune IgG or input from Caco-2 cell extracts. RNA levels in immunoprecipitates were determined by qRT-PCR. (E) The expression of miR-874 in Caco-2 cells was examined by miRNA RT-PCR after transfection with H19 and siH19. (F, G) Immunofluorescence and western blot analysis of AQP3 protein levels following treatment of Caco-2 cells with siH19, H19, pre-miR-874 and/or miR-874 inhibitor. $*P < 0.05$, $**P < 0.01$, $***P < 0.001$. N.S., not significant.

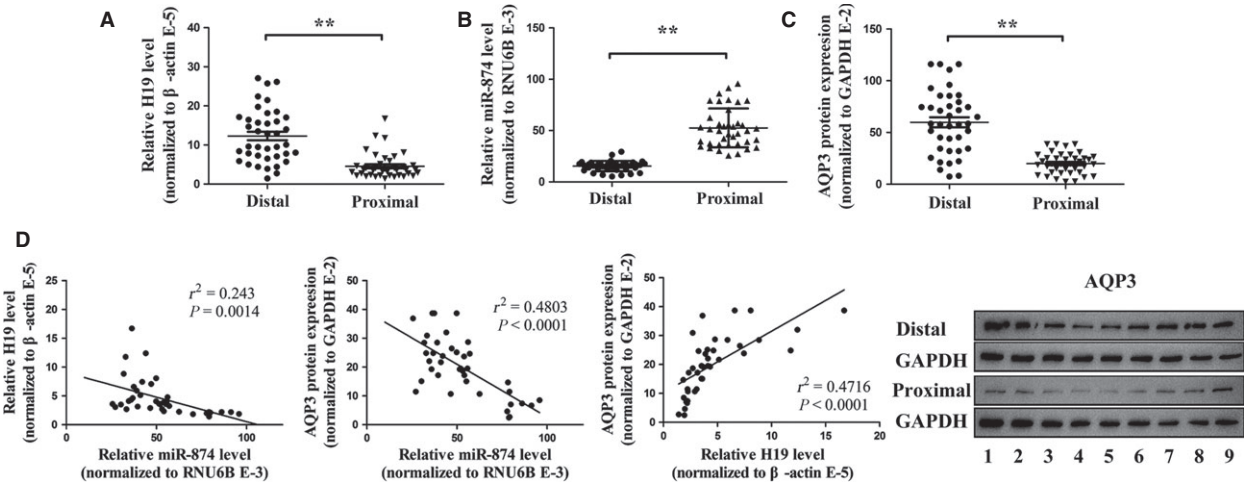

Fig. 2. Expression pattern of H19, miR-874 and AQP3 in adhesive small-bowel obstruction tissues. (A, B) qRT-PCR and miRNA RT-PCR were used to detect the expression of H19 and miR-874 in 39 pairs of proximal and distal mucous tissues from the lesion location, which were obtained from adhesive small-bowel obstruction patients who had undergone partial excision of the small bowel. (C) Western blot was used detect the expression of AQP3 in proximal and distal mucous tissues, and the protein expression of nine random matched samples is shown. (D) The scatter plots show the expression of H19, miR-874 and AQP3 in proximal mucous tissues. Linear regression analysis was used to measure the association between H19, miR-874 and AQP3.

levels of H19, miR-874 and AQP3 protein expression in proximal mucous tissues of diseased small bowel (Fig. 2D).

Changes of H19, miR-874 and AQP3 expression in a mouse model of intestinal ischaemia reperfusion injury

To further investigate the changes of H19, miR-874 and AQP3 expression in intestinal barrier dysfunction, we established a mouse model of intestinal ischaemia reperfusion injury. The results of qRT-PCR showed a time-dependent increase in miR-874 expression and a time-dependent decrease in H19 expression (Fig. 3A, B). The results of IHC and western blot showed that ischaemia reperfusion induced a time-dependent decrease of AQP3 protein expression after 15 min of SMA occlusion (Fig. 3C,D). Notably, we also found that the level of miR-874 expression was inversely related to H19 and AQP3 protein expression after 15 min of intestinal ischaemia (Fig. 3E,F).

Expression pattern of H19, miR-874 and AQP3 in Caco-2 cells under hypoxia and serum-free conditions

Intestinal barrier dysfunction was simulated *in vitro* by culturing Caco-2 cells under hypoxia and serum-free conditions for 0, 4, 8 and 12 h respectively. The results of qRT-PCR and western blot showed that the level of AQP3 protein and H19 expression were significantly reduced in a time-dependent manner in hypoxic and serum-free conditions (Fig. 4A,C). In contrast, the level of miR-874 was significantly increased with incubation time (Fig. 4B). Correlation analysis further suggested that the expression of H19, miR-874 and AQP3 showed a tendency towards correlation, but the results were not significant (data not shown).

Effect of H19 on TEER, paracellular permeability and *E. coli* translocation

The results showed that knockdown of H19 in Caco-2 cells caused an time-dependent increase in paracellular permeability compared with control groups, as measured by decreased TEER, increased LY permeability and *E. coli* translocation. In contrast, the paracellular permeability of the Caco-2 monolayer with overexpressed H19 showed a tendency to decrease. The results of rescue experiment showed that the negative regulation of Caco-2 cell monolayer paracellular permeability by H19 could be reverted by overexpression (H19/pre-miR-874) or knockdown (siH19/miR-874 inhibitor) of miR-874 (Fig. 5).

H19 alters the expression of the tight junction proteins

Tight junction proteins, including occludin, claudin-1, claudin-2, ZO-1, E-cadherin and beta-catenin were

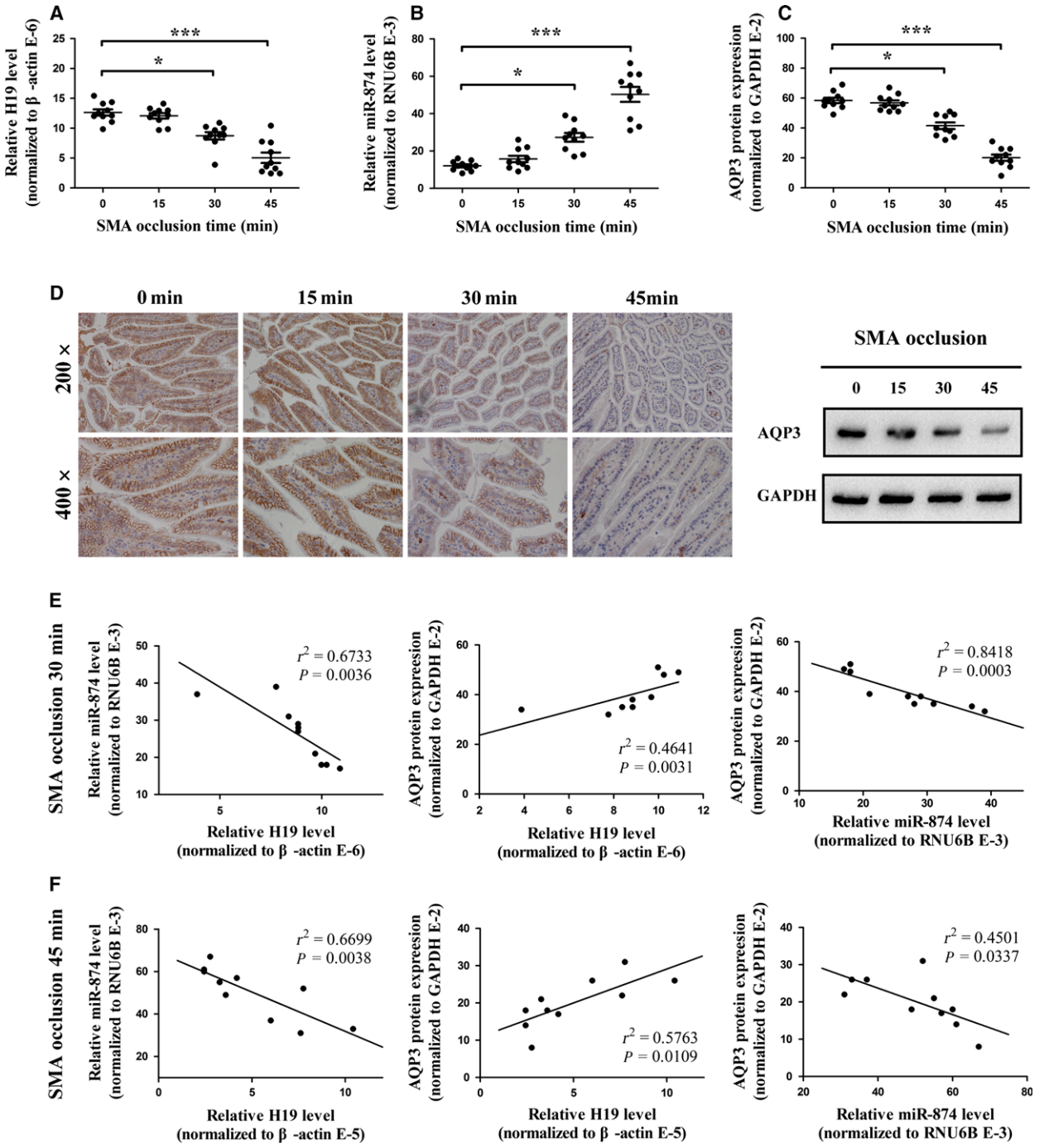

Fig. 3. Expression pattern of H19, miR-874 and AQP3 in a mouse model of intestinal ischaemia reperfusion injury. The superior mesenteric artery (SMA) was occluded for 0, 15, 30 and 45 min with 5 min reperfusion by using nontraumatic vascular clamps in the mouse intestinal ischaemia reperfusion injury model. Each group included 10 mice. (A, B) qRT-PCR and miRNA RT-PCR were used to detect the expression of H19 and miR-874 in each group. (C, D) Western blot and IHC were used to detect the expression of AQP3 in each group. (E, F) The scatter plots show the expression of H19, miR-874 and AQP3 in each group. Linear regression analysis was used to measure the association between H19, miR-874 and AQP3.

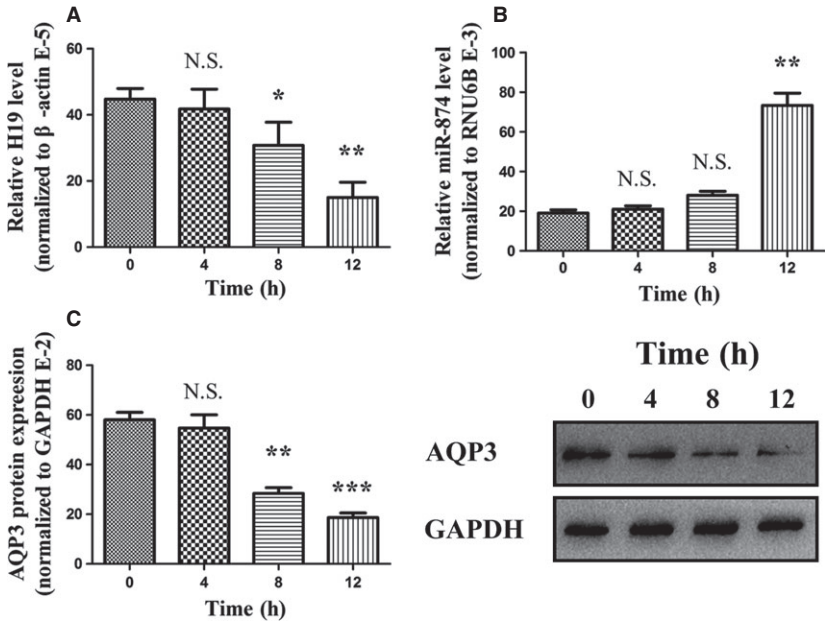

Fig. 4. Expression pattern of H19 miR-874 and AQP3 in a cellular hypoxia model. Caco-2 cells were incubated under hypoxia and serum-free conditions for 0, 4, 8 and 12 h. (A, B) qRT-PCR and miRNA RT-PCR were used to detect the expression of H19 and miR-874. (C, D) Western blot was used to detect the expression of AQP3.

detected by western blot in Caco-2 cells with both H19 overexpression and knockdown. The results showed that the expression of occludin and claudin-1 was significantly positively changed with H19 in Caco-2 cells. Expression of the other tight junction proteins did not change significantly (Fig. 6).

Discussion

Our previous study showed that AQP3 plays an important role in maintaining normal function of the intestinal barrier [10]. Furthermore, the effect and underlying mechanism of miR-874 on regulation of the intestinal barrier through targeting the 3′UTR of AQP3 was also confirmed [9]. Recently, a new regulatory mechanism was reported whereby lncRNA may function as competing endogenous RNA (ceRNA) to sponge miRNA, thereby modulating the derepression of miRNA targets and imposing an additional level of post-transcriptional regulation [25–28]. Inspired by the ceRNA regulatory network and our previous studies, we hypothesized that AQP3 protein may also be regulated by an lncRNA that serves as a ceRNA by sponging miR-874. In support of this notion, we employed bioinformatics analysis to predict putative lncRNA which might target miR-874. As expected, a putative lncRNA, lncRNA H19, which contains a putative 7-mer-binding motif binding site within miR-874, was found. RIP and luciferase assays validated the direct binding of the miR-874 response elements on the predicted lncRNA transcript. In addition, when H19 was overexpressed or knocked down in Caco-2 cells, the expression of miR-874 and AQP3 protein was observed to be negatively or positively regulated respectively. Taken together, these data are consistent with our hypothesis and indicate that H19 may interact with miR-874 to post-transcriptionally regulate the AQP3 protein.

The biological role of lncRNA H19 has been commanding attention for many years. Recent reports found that H19 may could function as a ceRNA for miRNA, antagonized its function [29,30]. In the present study, we investigated the expression pattern of H19, miR-874 and AQP3 in mucous tissues of adhesive small-bowel obstruction patients. The data showed that both H19 and AQP3 were expressed at higher levels in distal mucous tissues of lesion locations, with a lower expression of miR-874. Moreover, H19 expression was positively correlated with the expression of AQP3 and negatively correlated with the miR-874 in proximal mucous tissues of the lesion location. To further investigate the role of H19 in intestinal barrier dysfunction, a mouse model of intestinal ischaemia reperfusion injury was established. We examined the expression of H19, miR-874 and AQP3 in intestinal mucous tissues with different SMA

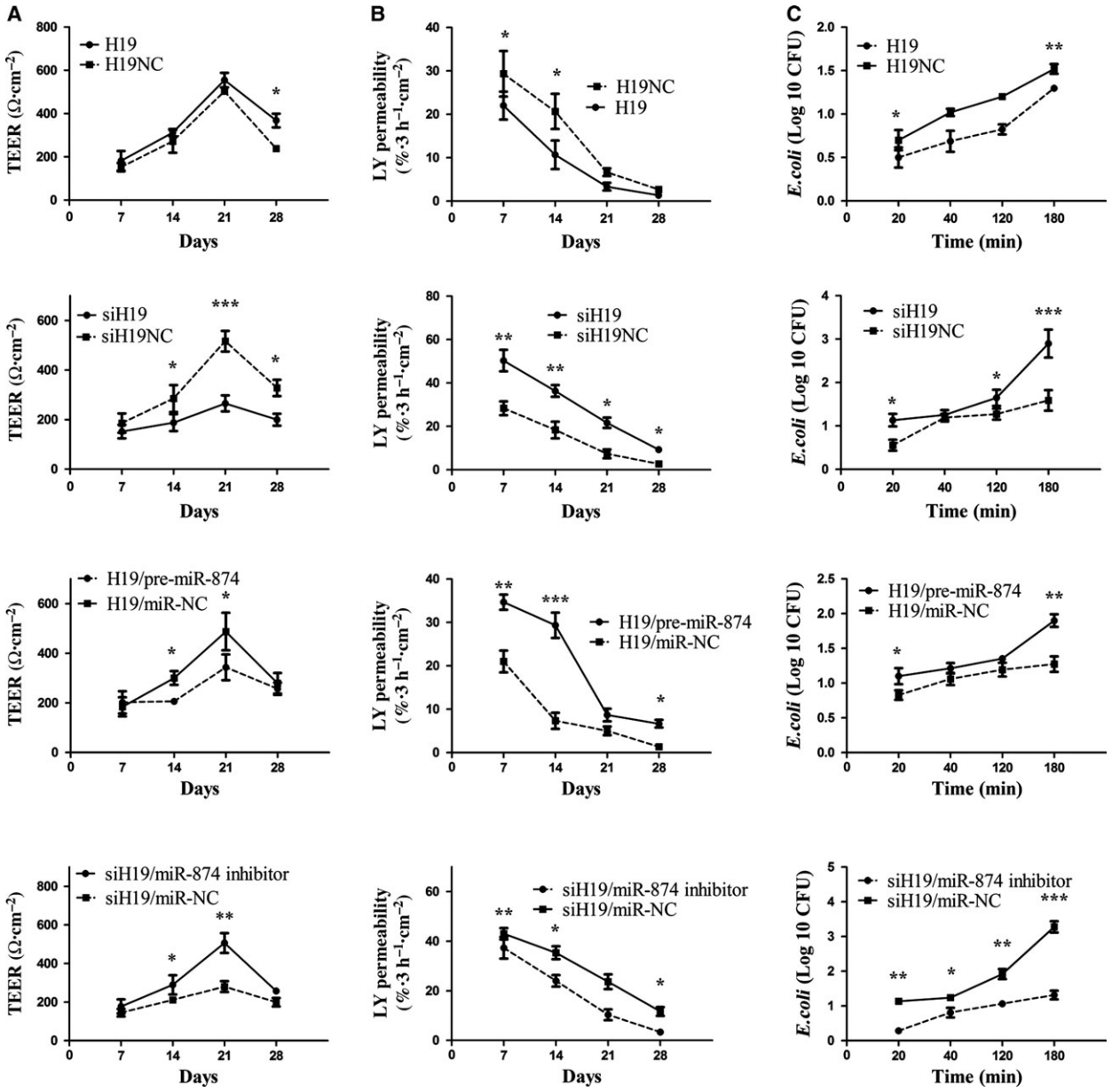

Fig. 5. H19 alters intestinal barrier function through miR-874. H19 and/or miR-874 were either overexpressed or knocked down in Caco-2 cells to generate H19, H19NC, siH19, siH19NC, H19/pre-miR-874, H19/miR-NC, siH19/miR-874 inhibitor and siH19/miR-NC. The formation of the monolayer of Caco-2 cells was monitored by measurements of the TEER (A), LY permeability (B) and bacterial translocation (C).

occlusion times. The results revealed that ischaemia reperfusion induced a time-dependent increase of miR-874 expression and a time-dependent decrease of H19 and AQP3 expression, and the level of miR-874 expression was inversely related to H19 and AQP3 protein expression. It confirmed the effect and underlying mechanism of H19 on regulation of the intestinal barrier.

To further define the effect of bacteria translocation and endotoxin following H19 knockdown and overexpression, we developed an *in vitro* cultured epithelial monolayer system, utilizing the Caco-2 cell line with different expressions of H19 and miR-874. Based on LY permeability, TEER and *E. coli* translocation results, it appears that the knockdown of H19 promoted the increase of paracellular permeability. In contrast, the level of paracellular permeability tends to be lower in the Caco-2 cell line with H19 overexpression compared with the control group. However, when we re-expressed miR-874 in the Caco-2 cells, the

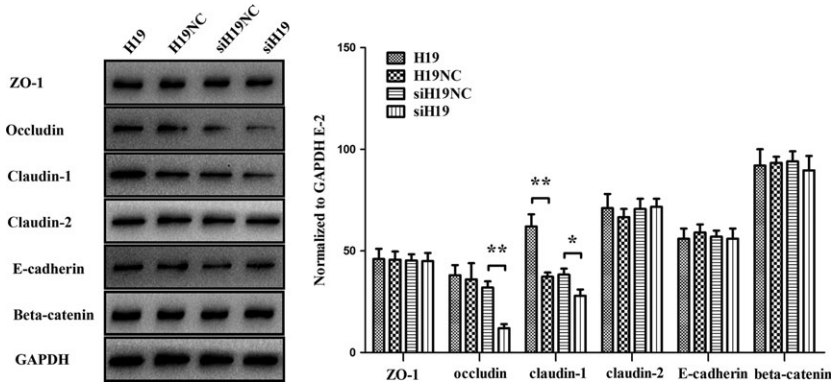

Fig. 6. H19 alters the expression of the tight junction proteins. The expression of tight junction proteins was detected by western blot.

transformation of paracellular permeability caused by H19 was restored. Moreover, our results showed two tight junction proteins, occludin and claudin-1, were significantly decreased in Caco-2 cells treated with siH19 compared with the negative control. All these findings further confirmed that H19 plays an important role in intestinal barrier dysfunction through targeting miR-874.

In summary, this study demonstrated that H19 down-regulation is a characteristic molecular change in intestinal barrier dysfunction, and we investigated the biological roles of H19, which may function as a ceRNA to regulate the expression of AQP3 through competition with miR-874. Further studies are required to assess the possibility of maintaining H19 expression to treat intestinal barrier dysfunction.

Author contributions

HX and ZX conceived the study. ZS performed most experiments. XZ and QZ performed immunofluorescence and PCR experiments. LY analysed the data, and ZS wrote the paper. All authors discussed the results and commented on the manuscript.

Acknowledgement

This work was funded by the Natural Science Foundation of Jiangsu Province (No. BK20141493) and the National Natural Science Foundation of China (81503160).

References

1 Turner JR (2009) Intestinal mucosal barrier function in health and disease. *Nat Rev Immunol* **9**, 799–809.
2 Julio-Pieper M, Bravo JA, Aliaga E and Gotteland M (2014) Review article: intestinal barrier dysfunction and central nervous system disorders—a controversial association. *Aliment Pharmacol Ther* **40**, 1187–1201.
3 Moore FA (1999) The role of the gastrointestinal tract in postinjury multiple organ failure. *Am J Surg* **178**, 449–453.
4 Swank GM and Deitch EA (1996) Role of the gut in multiple organ failure: bacterial translocation and permeability changes. *World J Surg* **20**, 411–417.
5 Besselink MG, van Santvoort HC, Renooij W, de Smet MB, Boermeester MA, Fischer K, Timmerman HM, Ahmed Ali U, Cirkel GA, Bollen TL *et al.* (2009) Intestinal barrier dysfunction in a randomized trial of a specific probiotic composition in acute pancreatitis. *Ann Surg* **5**, 712–719.
6 Bartel DP (2009) MicroRNAs: target recognition and regulatory functions. *Cell* **136**, 215–233.
7 Ohtsuka M, Ling H, Doki Y, Mori M and Calin GA (2015) MicroRNA processing and human cancer. *J Clin Med* **8**, 1651–1667.
8 Farh KK, Grimson A, Jan C, Lewis BP, Johnston WK, Lim LP, Burge CB and Bartel DP (2005) The widespread impact of mammalian MicroRNAs on mRNA repression and evolution. *Science* **5755**, 1817–1821.
9 Zhi Xiaofei, Tao Jinqiu, Li Zengliang, Jiang B, Feng J, Yang L, Xu H and Xu Z (2014) MiR-874 promotes intestinal barrier dysfunction through targeting AQP3 following intestinal ischemic injury. *FEBS Lett* **588**, 757–763.
10 Zhang W, Xu Y, Chen Z, Xu Z and Xu H (2011) Knockdown of aquaporin 3 is involved in intestinal barrier integrity impairment. *FEBS Lett* **585**, 3113–3119.
11 Wilusz JE, Sunwoo H and Spector DL (2009) Long noncoding RNAs: functional surprises from the RNA world. *Genes Dev* **23**, 1494–1504.
12 Salmena L, Poliseno L, Tay Y, Kats L and Pandolfi PP (2011) A ceRNA hypothesis: the Rosetta Stone of a hidden RNA language? *Cell* **146**, 353–358.
13 Liu XH, Sun M, Nie FQ, Ge YB, Zhang EB, Yin DD, Kong R, Xia R, Lu KH, Li JH *et al.* (2014) Lnc RNA

HOTAIR functions as a competing endogenous RNA to regulate HER2 expression by sponging miR-331-3p in gastric cancer. *Mol Cancer* **13**, 92–96.
14 Bartolomei MS, Zemel S and Tilghman SM (1991) Parental imprinting of the mouse H19 gene. *Nature* **6322**, 153–155.
15 Yang C, Tang R, Ma X, Wang Y, Luo D, Xu Z, Zhu Y and Yang L (2015) Tag SNPs in long non-coding RNA H19 contribute to susceptibility to gastric cancer in the Chinese Han population. *Oncotarget* **6**, 15311–15320.
16 Zhu M, Chen Q, Liu X, Sun Q, Zhao X, Deng R, Wang Y, Huang J, Xu M, Yan J *et al.* (2014) lncRNA H19/miR-675 axis represses prostate cancer metastasis by targeting TGFBI. *FEBS J* **281**, 3766–3775.
17 Wang J, Song YX and Wang ZN (2015) Non-coding RNAs in gastric cancer. *Gene* **560**, 1–8.
18 Ghazal S, McKinnon B, Zhou J, Mueller M, Men Y, Yang L, Mueller M, Flannery C, Huang Y and Taylor HS (2015) H19 lncRNA alters stromal cell growth via IGF signaling in the endometrium of women with endometriosis. *EMBO Mol Med* **8**, 996–1003.
19 Gao W, Zhu M, Wang H, Zhao S, Zhao D, Yang Y, Wang ZM, Wang F, Yang ZJ, Lu X *et al.* (2015) Association of polymorphisms in long non-coding RNA H19 with coronary artery disease risk in a Chinese population. *Mutat Res* **772**, 15–22.
20 Liu YL, Matsuzaki T, Nakazawa T, Murata S, Nakamura N, Kondo T, Iwashina M, Mochizuki K, Yamane T, Takata K *et al.* (2007) Expression of aquaporin 3 (AQP3) in normal and neoplastic lung tissues. *Hum Pathol* **1**, 171–178.
21 Matsuzaki T, Tajika Y, Ablimit A, Aoki T, Hagiwara H and Takata K (2004) Aquaporins in the digestive system. *Med Electron Microsc* **2**, 71–80.
22 Jiang B, Li Z, Zhang W, Aoki T, Hagiwara H and Takata K (2014) miR-874 Inhibits cell proliferation, migration and invasion through targeting aquaporin-3 in gastric cancer. *J Gastroenterol* **6**, 1011–1025.
23 Filipowicz W, Bhattacharyya SN and Sonenberg N (2008) Mechanisms of posttranscriptional regulation by microRNAs: are the answers in sight? *Nat Rev Genet* **9**, 102–114.
24 Izaurralde E (2012) Elucidating the temporal order of silencing. *EMBO Rep* **13**, 662–663.
25 Tuo YL, Li XM and Luo J (2015) Long noncoding RNA UCA1 modulates breast cancer cell growth and apoptosis through decreasing tumor suppressive miR-143. *Eur Rev Med Pharmacol Sci* **18**, 3403–3411.
26 Xing CY, Hu XQ, Xie FY, Yu ZJ, Li HY, Bin-Zhou, Wu JB, Tang LY and Gao SM (2015) Long non-coding RNA HOTAIR modulates c-KIT expression through sponging miR-193a in acute myeloid leukemia. *FEBS Lett* **15**, 1981–1987.
27 Tsang FH, Au SL, Wei L, Fan DN, Lee JM, Wong CC, Ng IO and Wong CM (2015) Long non-coding RNA HOTTIP is frequently up-regulated in hepatocellular carcinoma and is targeted by tumour suppressive miR-125b. *Liver Int* **5**, 1597–1606.
28 Gao Y, Meng H, Liu S, Hu J, Zhang Y, Jiao T, Liu Y, Ou J, Wang D, Yao L *et al.* (2015) LncRNA-HOST2 regulates cell biological behaviors in epithelial ovarian cancer through a mechanism involving microRNA let-7b. *Hum Mol Genet* **3**, 841–852.
29 Zhou X, Ye F, Yin C, Zhuang Y, Yue G and Zhang G (2015) The interaction between MiR-141 and lncRNA-H19 in regulating cell proliferation and migration in gastric cancer. *Cell Physiol Biochem* **36**, 1440–1452.
30 Wang SH, Wu XC, Zhang MD, Weng MZ, Zhou D and Quan ZW (2016) Long noncoding RNA H19 contributes to gallbladder cancer cell proliferation by modulated miR-194-5p targeting AKT2. *Tumour Biol*, doi:10.1007/s13277-016-4852-1.